Supporting Information

Article

Continuous-Flow Sunlight-Powered CO2 Methanation Catalyzed by γ-Al2O3-Supported Plasmonic Ru Nanorods

Jelle Rohlfs[1], Koen W. Bossers[1], Nicole Meulendijks[1], Fidel Valega Mackenzie, [1] Man Xu[1, 2], Marcel A. Verheijen[3,4], Pascal Buskens[1,5,*], and Francesc Sastre[1,*]

[1] The Netherlands Organisation for Applied Scientific Research (TNO), High Tech Campus 25, 5656AE Eindhoven, The Netherlands
[2] Optics Research Group, Delft University of Technology, Lorentzweg 1 (Building 22), 2628CJ Delft, The Netherlands
[3] Eurofins Materials Science, High Tech Campus 11, 5656AE Eindhoven, The Netherlands
[4] Department of Applied Physics, Eindhoven University of Technology, 5600MB Eindhoven, The Netherlands.
[5] Institute for Materials Research. Design and Synthesis of Inorganic Materials (DESINe), Hasselt University, Agoralaan Building D, B-3590 Diepenbeek, Belgium

* Correspondence: pascal.buskens@tno.nl; francesc.sastrecalabuig@tno.nl

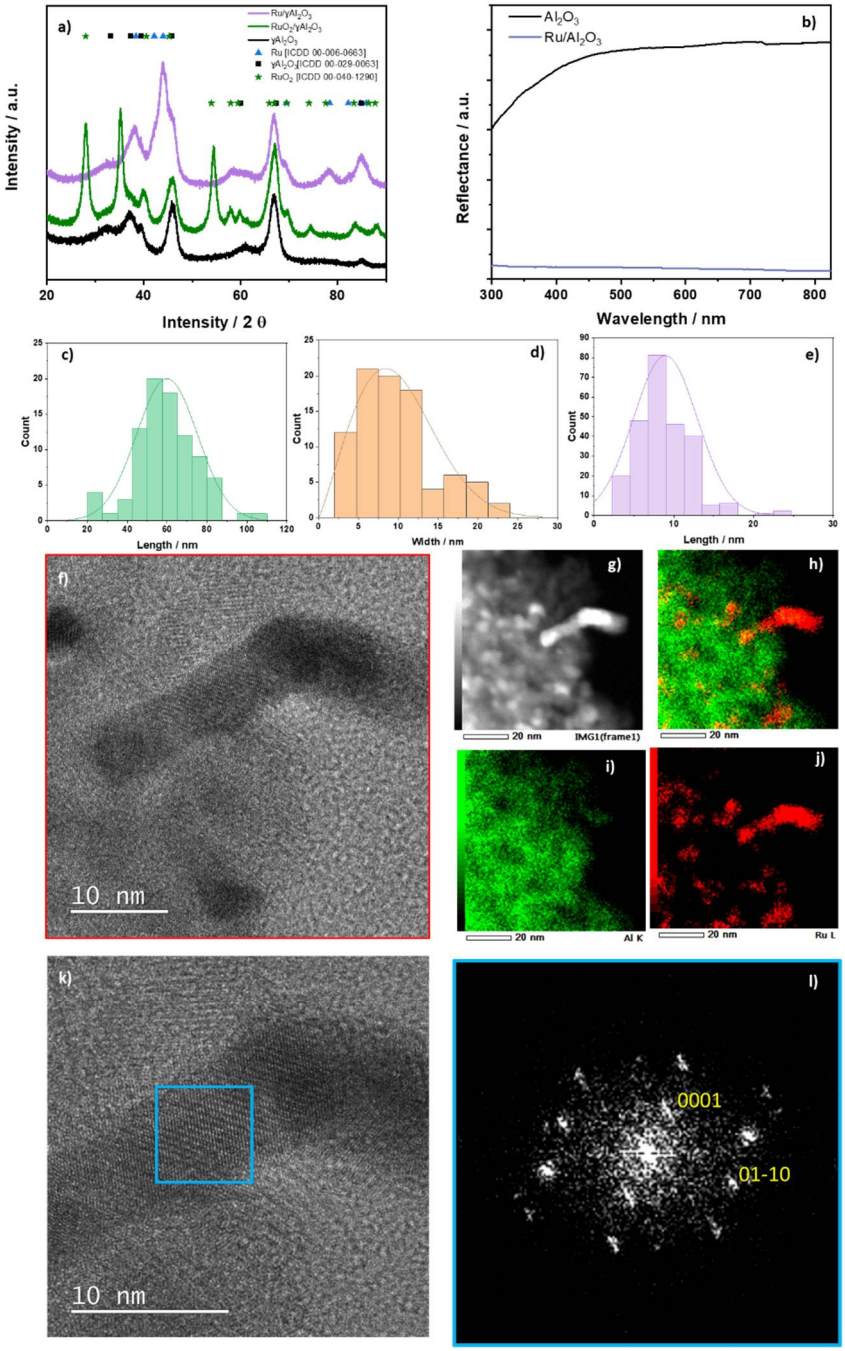

Figure S1. Optical and structural characterization of the Ru/ɣ-Al_2O_3 catalyst: **a)** XRD pattern of the Ru/ɣ-Al_2O_3 (purple line), RuO_2/ɣ-Al_2O_3 (green line) and ɣ-Al_2O_3 (black line) containing the characteristic peak positions for the corresponding Ru (blue triangles, ICDD 00-006-0663), RuO_2 (green triangles, ICDD 00-040-1290) and ɣ-Al_2O_3 (black squares, ICDD 00-029-0063) **b)** diffuse reflectance UV-vis spectra **c**) the size distribution histogram of the Ru NRs determined an average NR length of 59.8 nm, **d)** the size distribution histogram an average NR width of 9.9 nm**, e)** the size distribution histogram of the Ru spheres determined an average 8.9 nm , **f)** HRTEM image of Ru on ɣ-Al_2O_3 **g)** HAADF-STEM image**, h-j)** corresponding EDX elemental maps of Al (green) and Ru (red). **k)** HRTE images of a Ru nanorod. **l)** FFT pattern of the area selected in (k), corresponding to a <2-1-10> zone axis pattern of the hexagonal Ru crystal structure.

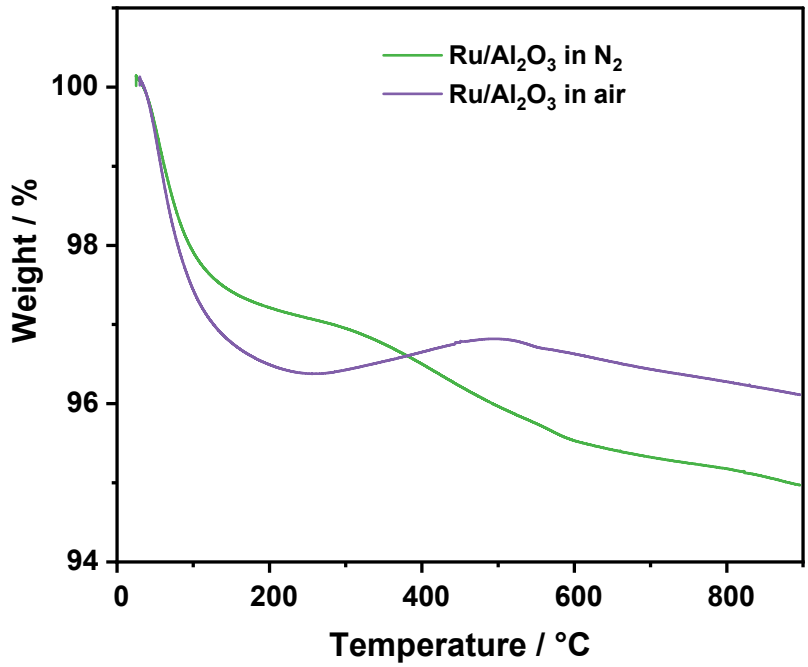

Figure S2. Thermogravimetric analysis for Ru/Al_2O_3 under N_2 or air atmosphere.

Equipment for the CO_2 photomethanation reactions

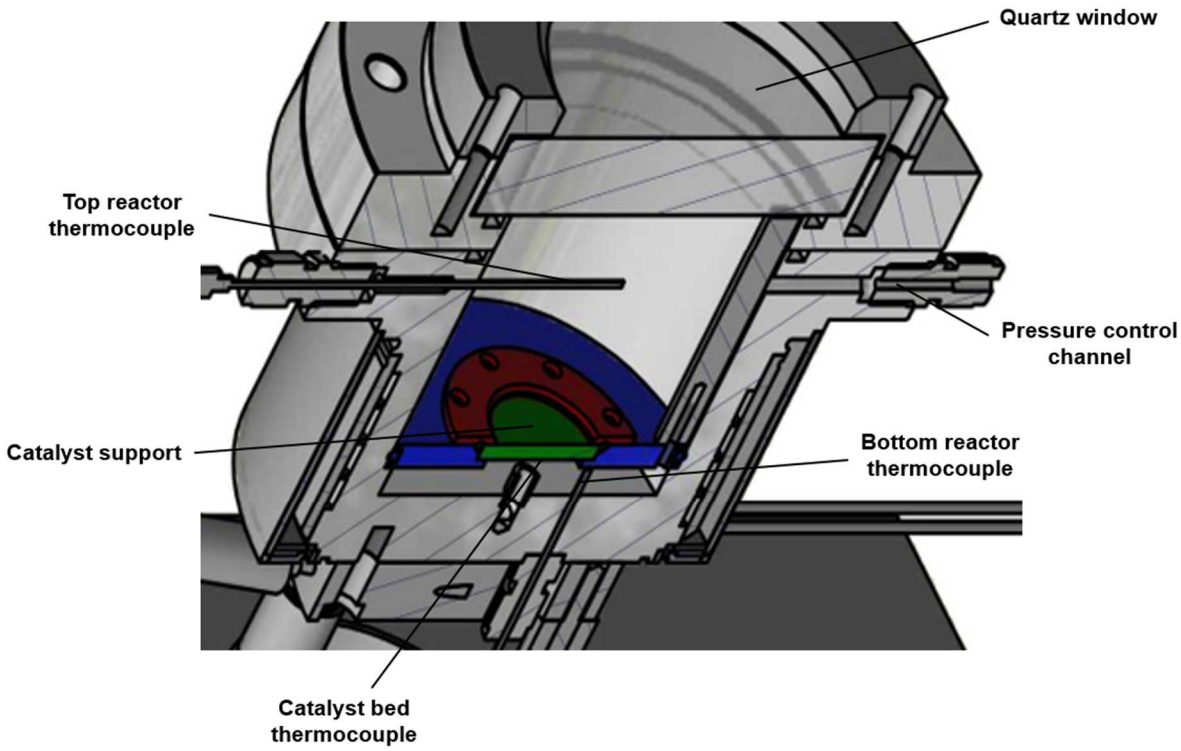

Figure S3. Schematic representation of the photoreactor.

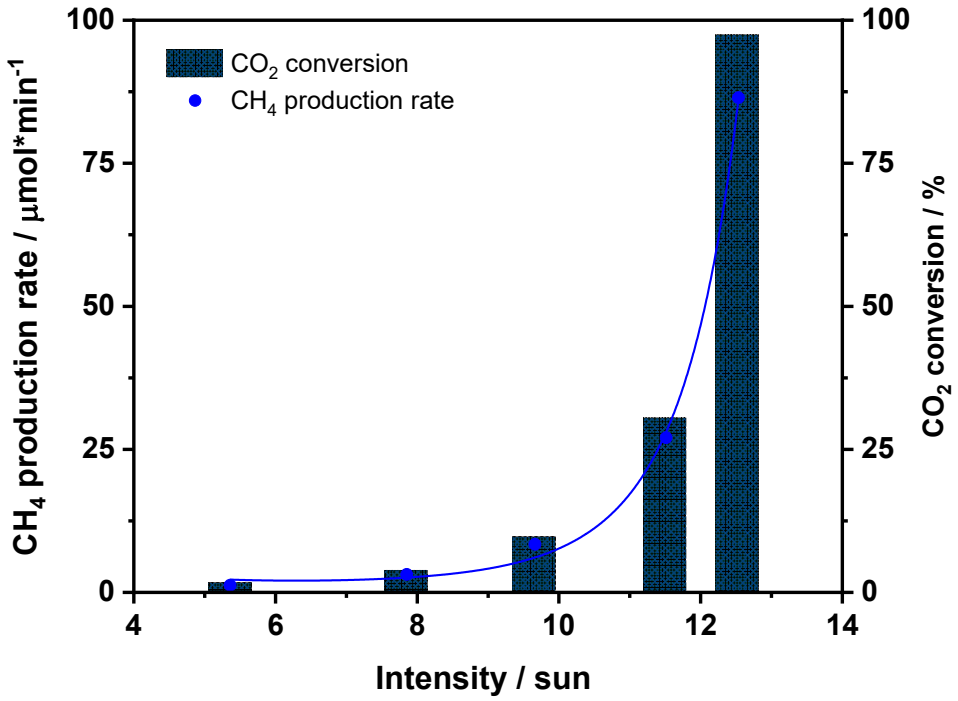

Figure S4. CH_4 production rate and CO_2 conversion as function of light intensity for the CO_2 photomethanation without external heating. Reaction conditions: mixture of H_2:CO_2:N_2 (4.5:1:1) with a flow of (9:2:2) ml·min^{-1} at 1.5 bar pressure (10wt% Ru/γ-Al_2O_3, 200 mg total catalyst mass, AM1.5 irradiance (1 sun = 1 kW·m^{-2})).

Equation for the (apparent) activation energy calculation

Arrhenius equation:

$$R_{CO} = A \cdot e^{\left(\frac{-E_a}{RT}\right)} \quad \text{(eq. S1)}$$

A = Pre-exponential factor.

E_a = Activation Energy.

R = Gas constant (8.314 $J \cdot K^{-1} \cdot mol^{-1}$).

T = Reaction temperature.

Table S1. Photocatalytic CH_4 production and reaction conditions

Ref	Catalyst	Year	Mode	Lamp		Irradiation		Reactor T	Catalyst T	Products	
				Power (W)	Type	Filters	Intensity (mW/cm^2)	(°C)	(°C)	CH_4	CO
[1]	Ru NPs/TiO_2	1987	Batch	--	--	Solar simulator	80	RT	90	10 $\mu mol \cdot h^{-1}$	--
[2]	Ni/SiO_2-Al_2O_3	2014	Batch	--	--	AM 1.5	--	RT	150	54.6 $mmol.g_{cat}^{-1}.h^{-1}$	94.9%CO_2 conv. 2.8% Selec.
[3]	Ru/AlO_3	2014	Batch	300	Xe	--	--	RT	300-400	95.75% CO_2 conv. 99.22% Selec.	95.75% CO_2 conv. 0.78% Selec.
[3]	Rh/$Al2O_3$	2014	Batch	300	Xe	--	--	RT	300-400	96.25% CO_2 conv. 99.48% Selec.	96.25% CO_2 conv. 0.52% Selec.
[3]	Ni/Al_2O_3	2014	Batch	300	Xe	--	--	RT	300-400	93.25% CO_2 conv. 99.04% Selec.	93.25% CO_2 conv. 0.25% Selec.
[4]	Rh/Al_2O_3	2017	Batch	--	LED	UV	3000	350	--	7 $\mu mol \cdot s^{-1}\ g^{-1}$	--
[5]	Cu_2O/Graphene	2017	Batch	300	Xe	--	200	250	--	14.93 $mmol.g_{Cu2O}^{-1}.h^{-1}$	--
[6]	RuO_2/i-Si-o	2018	Batch	300	Xe	--	2200	RT	170	4.4 mmol $g_{cat}^{-1}min^{-1}$	--
[7]	Ru/SiO_2	2018	Batch	300	Xe	--	2470	RT	150	2.8 mmol $g^{-1}min^{-1}$	
[8]	Ru NR/Al_2O_3	2019	Batch	300	Xe	AM 1.5	1010	25	221	52 $mmol.g_{Ru}^{-1}.h^{-1}$	--
[9]	Ru NPs/Al_2O_3	2020	Batch	300	Xe	AM 1.5	6.2	150	220	5.09 $mol.g_{Ru}^{-1}.h^{-1}$	--
[10]	Ni	2021	Batch	--	--	--	2000	RT	100	0.09 $mmol^{-1}.h^{-1}$	

[11]	Ni/SiO_2-Al_2O_3	2017	Flow	300	Xe	--	232.7	225	--	275 $\mu L \cdot g_{cat}^{-1} min^{-1}$ (3.5% CO_2 conversion)	--
[12]	Ru@LDHs	2017	Flow	300	Xe	--	1000	RT	350	277 mmol $g_{cat}^{-1} min^{-1}$	--
This publication	Ru NR/Al_2O_3		Flow	300	Xe	AM1.5	1450	25	204	792 $mmol \cdot g_{Ru}^{-1} \cdot h^{-1}$	

[1] K. R. Thampi, J. Kiwi, M. Grätzel, *Nature* **1987**, *327*, 506-508.
[2] F. Sastre, A. V. Puga, L. Liu, A. Corma, H. García, *JACS* **2014**, *136*, 6798-6801.
[3] X. Meng, T. Wang, L. Liu, S. Ouyang, P. Li, H. Hu, T. Kako, H. Iwai, A. Tanaka, J. Ye, *Angew Chem* **2014**, *126*, 11662-11666.
[4] X. Zhang, X. Li, D. Zhang, N. Q. Su, W. Yang, H. O. Everitt, J. Liu, *Nat Commun* **2017**, *8*, 14542.
[5] D. Mateo, J. Albero, H. García, *Energy Environ. Sci.* **2017**, *10*, 2392-2400.
[6] A. A. Jelle, K. K. Ghuman, P. G. O'Brien, M. Hmadeh, A. Sandhel, D. D. Perovic, C. V. Singh, C. A. Mims, G. A. Ozin, *Adv Energy Mater* **2018**, *8*, 1702277.
[7] P. G. O'Brien, K. K. Ghuman, A. A. Jelle, A. Sandhel, T. E. Wood, J. Y. Y. Loh, J. Jia, D. Perovic, C. V. Singh, N. P. Kherani, C. A. Mims, G. A. Ozin, *Energy Environ. Sci.* **2018**, *11*, 3443-3451.
[8] F. Sastre, C. Versluis, N. Meulendijks, J. Rodríguez-Fernández, J. Sweelssen, K. Elen, M. K. Van Bael, T. den Hartog, M. A. Verheijen, P. Buskens, *ACS Omega* **2019**, *4*, 7369-7377.
[9] R. Grote, R. Habets, J. Rohlfs, F. Sastre, N. Meulendijks, M. Xu, M. Verheijen, K. Elen, A. Hardy, M. van Bael, T. den Hartog, P. Buskens, *ChemCatChem* **2020**, *12*, 5618-5622.
[10] T. M. Steeves, A. P. Esser-Kahn, *RSC Advances* **2021**, *11*, 8394-8397.
[11] J. Albero, E. Dominguez, A. Corma, H. García, *Sustainable Energy & Fuels* **2017**, *1*, 1303-1307.
[12] J. Ren, S. Ouyang, H. Xu, X. Meng, T. Wang, D. Wang, J. Ye, *Adv Energy Mater* **2017**, *7*, 1601657.